Proceeding Series of the Brazilian Society of Computational and Applied Mathematics, v. 12, n. 1, 2026.

Trabalho apresentado no XLIV CNMAC, Fundação Getulio Vargas - Rio de Janeiro - RJ, 2025.

Proceeding Series of the Brazilian Society of Computational and Applied Mathematics

An Approximate Model for Planning Phase of Maritime SAR

Hengameh R. Dehkordi[1]
CMCC, UFABC, SP, Brazil

Abstract. This work applies advanced mathematical tools to address the planning phase of maritime Search and Rescue problems. We use Randers, Lorentz-Finsler, and Kropina metrics to predict the paths of survivors or debris after a shipwreck or an incident at sea.

Applying Finsler metric techniques to SAR models could enhance the accuracy of object drift predictions. Since Finsler metrics naturally arise in problems involving anisotropic media, such as ocean currents and wind, they are well-suited for optimizing drift predictions. To demonstrate the applicability of the proposed model in the planning phase of SAR problems, one example is implemented in MATLAB.

Keywords: Finsler Metric; SAR Problem; Geodesics; Total Drift.

1 Introduction

This study employs mathematical techniques to optimize path modeling for lost objects at sea, enhancing the planning of Search and Rescue (SAR) operations. Maritime SAR focuses on locating missing vessels, life rafts, or individuals in the water. These operations involve planning, searching, and rescue, which means defining the search area using resources to locate the target and assist an object in distress.

Approximately two-thirds of the planet is covered by water, and locating something lost at sea is a difficult challenge. We use Finsler geometry techniques to improve marine SAR operation (planning part), where the goal is to predict the drift of objects on the surface of water. The objects in question drift due to ocean currents, wind drift, wave drift, tidal forces, and other environmental variables that may be anisotropic, varying in speed and direction in different ocean parts.

Considering the specific circumstances of each search operation, the SAR team selects the most suitable search pattern. The six commonly used patterns include parallel tracks, creeping lines, expanding squares, sectors, barriers, and track lines [4]. Despite advancements in technology, there are situations where search and rescue operations rely on individuals scanning the sea with binoculars, revealing the limitations of existing methods[2]. Studying the SAR problem from a Finsler geometric perspective is useful because it provides a more comprehensive and accurate framework for modeling complex environments and optimizing paths under varying conditions. For instance, modeling object paths under specific perturbations is studied in [9]. We apply recent advances in mathematics and physics [5–8, 11] to provide the path and uncertainty areas of the lost object.

We introduce a Finsler metric framework for the SAR problem, which accounts for a non-uniform drift velocity field and inhomogeneous factors. This approach enables the modeling of both the search area and the potential paths of objects within an anisotropic sea environment. In

[1]hengameh.r@ufabc.edu.br
[2]https://www.wired.com/2014/03/flight-370-search/

DOI: 10.5540/03.2026.012.01.0245

real-world SAR scenarios, it is crucial to consider multiple possible movement directions, rather than assuming that the object follows only the total drift. Despite the dominance of the total drift, random effects, such as small-scale turbulence and chaotic sea dynamics, cause significant deviations. When the total force created by the current, wind, and wave is very strong, the movement of the object follows the dominant force direction. We will address these scenarios using the Kropina and Lorentz-Finsler metrics. When the total force is not strong, the path of the object is affected by the lateral drifts caused by multiple influencing factors. We associate a Randers metric with this scenario.

The novelty of this work is the application of geometric techniques to model the paths and uncertainty area of an object lost in water to improve the planning phase of SAR model techniques. The models process data from the SAR team, identify the appropriate metric, and generate predictions for the object's path and associated uncertainty regions.

2 Mathematics Background

Let M be an open subset of $\mathbb{R}^2$, with $p = (x, y)$ representing an arbitrary point in M. We denote the tangent space to M at p by $T_pM \approx \mathbb{R}^2$, and the tangent bundle with TM. We employ the standard basis $\{\frac{\partial}{\partial x}, \frac{\partial}{\partial y}\}$ for T_pM and express each tangent vector as $V = (v_1, v_2)$.

A Riemannian metric on M is a smooth function h that assigns an inner product $h_p : T_pM \times T_pM \to \mathbb{R}$ to each point $p \in M$. A Finsler metric on M is a function $F : TM \to [0, \infty)$ that is smooth on $TM \setminus \{0\}$, positive homogeneous of degree one; $F(x, \mu V) = \mu F(x, V)$ for all $\mu > 0$, and the determinant of its Hessian matrix, $[g^V_{ij}(p)]$,

$$g^V_{ij}(p) = \frac{1}{2} \frac{\partial^2 F^2}{\partial v_i \partial v_j}(x, V), \tag{1}$$

is positive definite.

A smooth curve $\gamma : [0, 1] \to M$ in the Finsler space (M, F) is a geodesic if it locally minimizes the time taken to traverse between any two nearby points on $\gamma([0, 1])$. In a Finsler space (M, F), the Finsler geodesics $\gamma(t)$ are solutions to the following system of differential equations:

$$\ddot{\gamma}_r(t) = -\gamma^{jk}_r(\gamma, \dot{\gamma})\dot{\gamma}_j(t)\dot{\gamma}_k(t), \quad r = 1, 2, \tag{2}$$

where

$$\gamma^{jk}_r = \frac{1}{2} g^{rl}_V \left(\frac{\partial g^V_{lk}}{\partial x^j} + \frac{\partial g^V_{lj}}{\partial x^k} - \frac{\partial g^V_{kj}}{\partial x^l} \right), \quad r = 1, 2, \tag{3}$$

with $[g^V_{rj}]$ denoting the matrix of the second fundamental form of F and $[g^{rj}_V]$ its inverse [13]. Given two vectors $V, U \in T_pM$, U is F-orthogonal to V, $V \underset{F}{\perp} U$, if $g^V_{ij}(p)(V, U) = 0$.

2.1 Zermelo's Navigation Problem

The Zermelo's navigation problem, introduced by Zermelo in 1931 [15], is an optimal control problem that seeks to determine the time-optimal path for a ship to travel from point A to point B in the presence of external forces, like wind or current, denoted by W. The vessel has a constant speed relative to the medium and given initial conditions and seeks the single optimal path which is determined by solving differential equations. Having the fixed initial and end points the uncertainty is minimal. A SAR problem aims at maximizing the probability of detection (or minimizing the time to locate) a lost object or person over a search area. The SAR problem deals

DOI: 10.5540/03.2026.012.01.0245

with probabilistic distributions of where the object might be, influenced by environmental drift (current, wind, waves) and uncertainty in the object's paths.

Zermelo solved Zermelo's problem in Euclidean space, that is under homogeneous environmental factors. Later, Shen [12] explored the problem in Riemannian space, that is inhomogeneous environmental factors, for the case where the wind´s magnitude is less than 1. Specifically, given a Riemannian metric h and a vector field W representing the wind with $h(W,W) < 1$, Shen showed that the following metric which is called a Randers metric provides time-minimizing trajectories:

$$F(V) = \frac{\sqrt{h^2(W,V) + \lambda h(V,V)}}{\lambda} - \frac{h(W,V)}{\lambda}, \tag{4}$$

where $\lambda = 1 - h(W,W)$. Sabau [11] extended this work to the case where $||W|| = 1$, proving that the navigation problem can be solved using a metric:

$$F(V) = \frac{h(V,V)}{2h(V,W)}, \tag{5}$$

defined on the conic domain $A = \{V \in TM : h(V,W) > 0\}$ which is called a Kropina metric. Finally, for the strong wind case, $||W|| > 1$, Javaloyes [8] showed that the solution to Zermelo's problem is given by the Lorentz-Finsler metrics

$$F(V) = \frac{1}{\lambda}(\pm\sqrt{\lambda h(V,V) + h^2(W,V)} - h(W,V)), \tag{6}$$

defined on the set $A = \{V \in TM : \lambda < 0;\ \lambda h(V,V) + h^2(W,V) > 0;\ h(W,V) > 0\}$.

The next section provides some discussion on SAR problem and demonstrates how Finsler metrics model the trajectories of the lost object.

3 Search and Rescue Problem

The key components in SAR models are wind, current, and wave-induced drifts [10]. The wind causes the object to drift downwind and the magnitude of this drift depends on the wind speed. Ocean currents carry the object in a specific direction, independent of the wind, and can significantly influence the drift path. Waves can cause additional movement of the object, especially if it is partially submerged or has interaction with the sea surface.

3.1 Leeway Models

A leeway model is a mathematical or empirical tool used in maritime SAR to predict the wind-induced drift of objects or persons in the water. It occurs when the wind pushes the object off its intended or natural path, causing it to move downwind. Leeway models are critical for estimating the drift path of search objects. The process varies depending on whether the object is a person, a vessel, or debris [1, 2]. Leeway drift, $\alpha\mathbf{V}_{\text{wind}}$, is typically calculated using empirical formulas, field observations, or tracking methods. Here, α is the Leeway Coefficient which depends on factors such as the object's geometry, exposure to wind, and environmental conditions, and may vary from 0.5% to 3%. In SAR modeling, the total drift velocity, $\mathbf{V}_{\text{d}}$, is calculated as: $\mathbf{V}_{\text{d}} = \mathbf{V}_{\text{current}} + \mathbf{V}_{\text{wave}} + \alpha\mathbf{V}_{\text{wind}}$ where $\mathbf{V}_{\text{current}}$ is surface current velocity, $\mathbf{V}_{\text{wave}}$ is stokes drift, i.e. wave-induced motion, and $\alpha\mathbf{V}_{\text{wind}}$ is leeway drift. There are several sources to collect wind, wave, and current data. For instance for wind and wave factors, the SAR team may use the satellites and for current speed and direction, the team may use the tide gauges [3].

The SAR model predicts the drift path of the object and the search area which is an ellipse. The drift path is calculated based on $\mathbf{V}_{\text{d}}$ and the ellipse which is called the uncertainty ellipse

is due to the uncertainty. The major axis is along the drift direction and represents greater uncertainty due to wind fluctuations and the minor axis accounts for lateral spread caused by wave and current variability. Ellipses grow larger over time due to increasing prediction errors. SAR assets (helicopters, ships, drones) prioritize the search area based on the center of the ellipse because it has the highest probability location. Then the major axis direction because it has more likely drift, and then the entire ellipse boundary to account for errors. If the precise location is unknown, the SAR team uses expanding square search, and if the ellipse is large it uses parallel track search, and if the object was last seen near a known location, the team uses sector search. As environmental conditions change, SAR models can be updated to refine the search area.

3.2 Finsler Approach to Maritime SAR

Objects at sea experience more than just drift. Although the total drift, $\mathbf{V}_{\mathrm{d}}$, dominates the overall movement, several random and physical factors cause deviations. For instance, if an object was moving before drifting (e.g., a person falling overboard), it does not immediately align with the drift. Additionally, different objects respond differently to wind and currents depending on their shape, weight, and buoyancy. Objects also tend to bob and shift due to wave-induced motion, creating small, unpredictable variations. As a result, while the object generally follows the drift direction, these deviations lead to a spreading effect, forming an uncertain region around the expected drift path. In SAR operations, many of these complex factors are simplified, with primary attention given to wind, waves, and currents [14].

To address a SAR problem, this work uses Randers (4), Kropina (5), and Lorentz-Finsler (6) metrics to approximate the paths of the object and the uncertain area. To model the problem, we first represent the total drift as a vector field W, which accounts for anisotropic drift effects, and the Riemannian metric h captures isotropic environmental factors. To derive the associated Riemannian metric h, we consider a scenario in which the total drift is zero—that is, there is no dominant forcing from wind, currents, or waves. Under these isotropic conditions, the lost object's motion is affected primarily by random, small-scale influences such as micro-currents, turbulence, wave action, and the object's intrinsic properties. These effects lead to an expanding uncertainty region over time, typically modeled as a circular or elliptical area. For further discussion on uncertainty regions under isotropic conditions, see [3]. These circular and elliptical areas lead to the Euclidean metric $h = \frac{dx^2+dy^2}{R^2}$, where R is the radius of the circle, and Riemannian metric

$$h = (\frac{\cos^2\theta}{a^2} + \frac{\sin^2\theta}{b^2})dx^2 + (\frac{\sin^2\theta}{a^2} + \frac{\cos^2\theta}{b^2})dy^2 + 2(\frac{1}{b^2} - \frac{1}{a^2})\sin 2\theta dxdy, \tag{7}$$

where a and b are major and minor axes of the ellipse, respectively, and θ is the angle that total drift makes with the east. Depending on the magnitude of the drift vector W relative to the Riemannian metric h, we obtain different Finslerian structures. Specifically, when $|W|_h < 1$, the metric is of Randers type, see (4); when $|W|_h = 1$, it becomes a Kropina metric, see (5); and when $|W|_h > 1$, the resulting metric is Lorentz-Finsler, see (6).

Once we determine the appropriate Finsler metric, the trajectories of the objects are given by curves $\gamma : [0, T] \to M$ which solve the geodesic equations (2) under the initial conditions $F(\gamma') = 1$, $\gamma'(0)$ makes angle from 0 to 2π with total drift, and $\gamma(0)$ being the object's initial location. If the object's initial position is uncertain, we define a potential starting region S bounded by a smooth curve $\beta(s)$, where $\beta([a, b])$ encloses S. In this case, the geodesic initial conditions are $F(\gamma') = 1$, $\gamma(0) = \beta(s)$, for some $s \in [a, b]$, and $\gamma'(0)$ is F-orthogonal to $\beta'(s)$. The uncertain area at time τ consists of the points $\{\gamma(\tau)\}$.

Next section provides one example analyzing survivor drift paths and uncertainty regions in maritime SAR.

DOI: 10.5540/03.2026.012.01.0245

4 Example

When an airplane crashes, the Rescue Coordination Center considers the line segment connecting the point of departure to the intended destination, which represents the planned flight path. When the departure point and the pretended destination are far from each other, the path of the plane might be a part of the great circle of the earth or a curved path, that is the geodesic of the space. This trajectory may be utilized to focus search efforts along the anticipated route of the aircraft. This approach facilitates the organization and optimization of the search process, enabling teams to systematically survey the area where the aircraft is most likely to be located. In the context of search operations, it is crucial to identify the region of highest probability. This example employs data provided by the SAR team to determine an appropriate metric. Through the analysis of object trajectories and uncertainty regions, one can enhance conventional search techniques—such as square search, sector search, and creeping line—resulting in a more efficient search strategy.

We consider an airplane crash occurring over the ocean, 5 km off the coast of Buenos Aires, Argentina. SAR teams have identified five locations where survivors may be present. Our objective is to analyze the potential drift trajectories of rescuers wearing life jackets, accounting for local wind, currents, wave patterns, and environmental constraints at each location. By recognizing the patterns, SAR teams can concentrate their efforts on high-probability areas, thereby optimizing resource allocation and enhancing the likelihood of successful rescues.

Fig. 1a shows the map of the location along with the currents, confirming that the vector fields considered in this example correspond to several real-world scenarios, where the current plays a dominant role in most cases [3]. Figs.1b to 1f provide the trajectories and the information on the total drift W and the axes and angle of the ellipse. The black arrows indicate dominant external forces, including wind, wave, and ocean currents. To analyze the cases, we associated Randers metrics with Figs. 1b, 1d, and 1e. A Kropina metric was associated with Fig. 1d, while for Fig. 1e, we used a Lorenz-Finsler metric. To derive the formulas for each metric, one can substitute the data provided in the figure captions into equations (4)-(6). To obtain the geodesic system equations, the equations (2) should be solved.

Fig. 1b illustrates the rotational drift dynamics when the initial positions form a region rather than a single point. The trajectories exhibit a spiraling motion rather than a strictly circular pattern, suggesting the influence of external forces such as currents, wind, or variable water conditions. The presence of an asymmetric drift indicates that a purely circular search strategy may not be effective. If a square search pattern is to be implemented, adjustments must be made to account for the non-uniform flow and directional drift observed in the figure.

Fig. 1c illustrates the dispersion of survivor trajectories under the influence of a uniform total drift vector. The spread of trajectories results from variations in local conditions, including turbulence and individual movement factors. The asymmetry in the model indicates that survivors are primarily transported in one direction while exhibiting divergence. This suggests that SAR operations should incorporate non-linear drift effects, adapting search strategies to account for the expanding region of potential survivor locations rather than relying on linear projections. For this case, an adjustment of the parallel search pattern might be useful.

Fig. 1d visualizes the model of survivor trajectories within a region characterized by complex drift patterns, specifically highlighting areas with multiple rotational drifts. The concentration of trajectories in certain directions suggests areas of higher probability for locating survivors.

Figs.1e and 1f model the trajectories under stable total drift. In Fig.1f, the total force is twice the Fig.1e. The areas with accumulated dots likely represent zones with a higher probability of survivor presence, making them crucial for prioritizing search efforts. In contrast, regions without dots may indicate lower likelihoods of survivor presence.

DOI: 10.5540/03.2026.012.01.0245

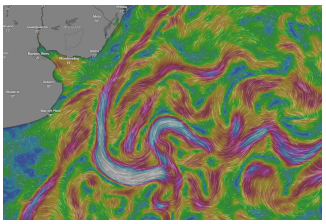

(a) The current. Source: windy.com.

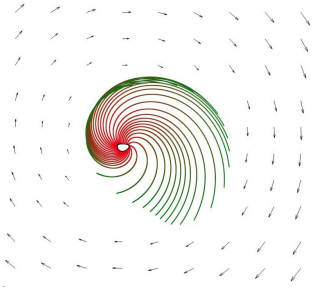

(b) $W = (y-3, 1-x), a = b = 5.3, \theta = \frac{\pi}{9}$.

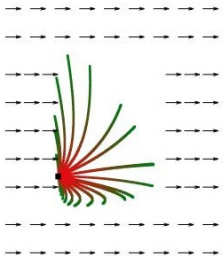

(c) $W = (1.4, 0), a = 2.8, b = y + 3, \theta = \frac{\pi}{9}$.

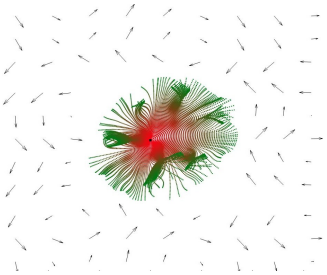

(d) $W = (cosy, sinx), a = 2.8, b = 2.1, \theta = \frac{\pi}{6}$.

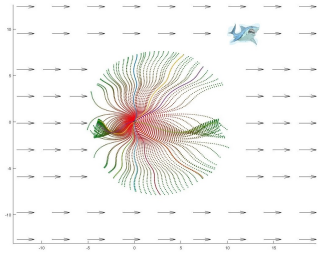

(e) $W = (0, 0.5), a = 1.8, b = 1.3, \theta = 1 - x$.

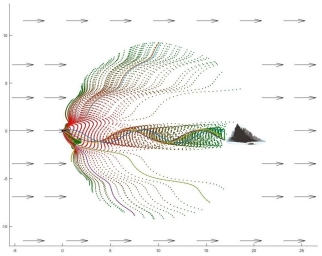

(f) $W = (0, 1), a = 2.5, b = 1.5, \theta = 1 - x$.

Figure 1: Potential paths for rescuers in different situations. Source of figures (b)-(f): own authorship.

5 Final Remarks and Conclusion

This work approached the maritime search and rescue problem from a geometric perspective, incorporating data provided by SAR teams into mathematical models that describe the object's trajectories and uncertainty regions. SAR planning involves predicting drift trajectories and selecting appropriate search patterns. By the application of Finsler metrics, we computed geodesics that account for environmental anisotropies, resulting in a more realistic model for path optimization. Consequently, the Finsler-based approach enhances the planning phase and improves the efficiency of risk management strategies in SAR operations.

We analyzed the problem's anisotropic and homogeneous properties using Randers, Kropina, and Lorentz-Finsler metrics. Randers metric was applied to model mild perturbations, while Kropina and Lorentz-Finsler metrics captured the effects of stronger drifts. An interesting direction for future research is the incorporation of time-dependent drifts, which require working with lightlike geodesics—a topic beyond the scope of this study but promising for further exploration.

Acknowledgment

This study was financed by FAPESP, Process Numbers 2022/15371-3.

References

[1] A. A. Allen. **The leeway of Cuban refugee rafts and a commercial fishing vessel**. Tech. rep. US Coast Guard, Office of Research and Development, 1996.

[2] E. Anderson, A. Odulo, and M. Spaulding. **Modeling of Leeway drift. US Coast Guard Research and Development Center**. Tech. rep. Report No. CG-D-06-99, 1998.

[3] Ø. Breivik and A. A. Allen. "An operational search and rescue model for the Norwegian Sea and the North Sea". In: **Journal of Marine Systems** 69.1-2 (2008), pp. 99–113.

[4] Coast Guard Washington DC. **US Coast Guard Addendum to the United States National Search and Rescue Supplement (NSS) to IAMSAR**. Tech. rep. 2009.

[5] H. R. Dehkordi. "Applications of Randers geodesics for wildfire spread modelling". In: **Applied Mathematical Modelling** 106 (2022), pp. 45–59.

[6] H. R. Dehkordi, M. Richartz, and A. Saa. "Wind-Finslerian structure of black holes". In: **Physical Review D** 112.2 (2025), p. 024004.

[7] H. R. Dehkordi and A. Saa. "Huygens' envelope principle in Finsler spaces and analogue gravity". In: **Class. Quantum Grav.** 36.8 (2019), p. 085008.

[8] M. A. Javaloyes, E. Pendás-Recondo, and M. Sánchez. "An Account on Links Between Finsler and Lorentz Geometries for Riemannian Geometers". In: Springer, 2023, pp. 259–303.

[9] P. Kopacz. "Application of planar Randers geodesics with river-type perturbation in search models". In: **Appl. Math. Model.** 49 (2017), pp. 531–553.

[10] S. Rangarajan and C. H. Mehta. "Search area analysis of exploration drilling for hydrocarbons". In: **Geophysics** 45.1 (1980), pp. 94–108.

[11] S. V. Sabau, K. Shibuya, and R. Yoshikawa. "Geodesics on strong Kropina manifolds". In: **European Journal of Mathematics** 3 (2017), pp. 1172–1224.

[12] Z. Shen. "Finsler metrics with K= 0 and S= 0". In: **CJM** 55.1 (2003), pp. 112–132.

[13] Z. Shen. **Lectures on Finsler geometry**. World Scientific, Singapore, 2001.

[14] J. Wu, L. Cheng, and S. Chu. "Modeling the leeway drift characteristics of persons-in-water at a sea-area scale in the seas of China". In: **Ocean engineering** 270 (2023), p. 113444.

[15] E. Zermelo. "Über das Navigationsproblem bei ruhender oder veränderlicher Windverteilung". In: **Zeitschrift für Angewandte Mathematik und Mechanik** 11.2 (1931).

